Electronic Properties of The Mg_2Si Thermoelectric Material Investigated by Linear-Response Density-Functional Theory

P. Boulet,[1] M. J. Verstraete,[2] J.-P. Crocombette,[3] M. Briki,[4] and M.-C. Record[5]

[1] *Université Aix-Marseille I II et III, Laboratoire Chimie Provence, UMR-CNRS 6462, Avenue Escadrille Normandie-Niemen, 13397 Marseille cedex 20, France**

[2] *Département de Physique, Université de Liège, B-4000 Liège, Belgium*

[3] *CEA, Saclay, DEN/SRMP, 91191 Gif-sur-Yvette Cedex, France*

[4] *Université Aix-Marseille I, II et III, Laboratoire Chimie Provence, UMR-CNRS 6462, Avenue Escadrille Normandie-Niemen, 13397 Marseille cedex 20, France*

[5] *Université Aix-Marseille III, Institut Matériaux Microélectronique Nanosciences de Provence, UMR-CNRS 6242, case 142, Avenue Escadrille Normandie-Niemen, 13397 Marseille Cedex 20, France*

Abstract

This paper presents Density-Functional Perturbation Theory (DFPT) calculations on the electronic, vibrational, and electron-phonon (EP) coupling properties of the Mg_2Si thermoelectric compound. The DFPT yields very satisfactory results for the electronic and vibrational properties when compared to experiment. Regarding the EP interactions, as far as we know, they have never been reported so far. We show that the EP interactions in Mg_2Si mainly involve the silicon atom. This result explains the improvement of the thermoelectric properties of Mg_2Si using a solid solution $Mg_2Si_{1-x}A_x$, where A is a heavier atom than Si. By guiding the choice of the substitution site, the study of the EP coupling properties could be used in the search of new thermoelectric materials based on solid solutions.

PACS numbers: 63.20.dk,63.20.kd,71.15.Mb,72.15.Eb

Keywords: Ab initio, electron-phonon interaction, thermoelectricity, silicide compounds, Mg_2Si

I. INTRODUCTION

For about two decades, needs for new sources of energy have made research on thermoelectric materials regaining interest. Among these materials, silicide compounds are promising ones for high temperature applications[1] (500-800 K). The efficiency of a thermoelectric material is measured by its figure of merit $ZT = \frac{S^2\sigma}{\kappa}T$, where S is the Seebeck coefficient, σ is the electrical conductivity, κ is the thermal conductivity, and T is the temperature. ZT can then reach high values when the thermopower $S^2\sigma$ is high and when κ is small. ZT is a dimensionless figure, and good thermoelectric materials are characterized by $ZT \geq 1.0$. Both an electronic and lattice conductivity contribution participate to the total thermal conductivity, and in virtue of the Wiedemann-Franz law, the electronic thermal conductivity and the electrical one are related to one another. Since the processes of electrical and electronic thermal conductivities in materials are related to the electron-phonon (EP) interaction, the comprehension of the EP coupling is desired to understand the behaviour of the material and to improve its thermoelectric properties. The work presented in this paper is mainly devoted to the theoretical study of the EP coupling in the Mg_2Si silicide compound. Electrical and electronic thermal conductivities were also calculated.

II. LITERATURE DATA

Mg_2Si crystallizes in a face centered cubic (FCC) Bravais lattice with primitive translation vectors $\mathbf{a} = a(0, \frac{1}{2}, \frac{1}{2})$, $\mathbf{b} = a(\frac{1}{2}, 0, \frac{1}{2})$ and $\mathbf{c} = a(0, \frac{1}{2}, \frac{1}{2})$ where a is the lattice parameter which equals to 0.635 nm. The structure symmetry of Mg_2Si is O_h^3, the corresponding space group is $Fm\bar{3}m$ (group number 225)[2]. Three in-

equivalent sites can be specified in the irreducible unit cell, namely Si: $a(0,0,0)$, Mg: $a(\frac{1}{4},\frac{1}{4},\frac{1}{4})$, and Mg: $a(\frac{3}{4},\frac{3}{4},\frac{3}{4})$. Mg_2Si belongs to the antifluorite structure family.

Elastic constants and bulk modulus of Mg_2Si have been given in Ref.[3]. The values are $C_{11} = 126$ GPa, $C_{12} = 26$ GPa, $C_{44} = 48.5$ GPa, and $B = 49$ GPa.

The electronic and vibrational properties of Mg_2Si have been widely studied in the literature.

Mg_2Si is a n-type semi-conductor with indirect gap of energy 0.66–0.78 eV ($\Gamma_v \rightarrow X_c$)[4–6]. The direct gap of Mg_2Si was determined by Vazquez *et al.* using electroreflectance experiment, and it amounts to 2.27 eV ($\Gamma_v \rightarrow \Gamma_c$)[7]. Pseudopotential[8], density-functional theory (DFT)[9], and GW[10] methods were used to calculate electronic properties of Mg_2Si. The reported data are gathered in Table I. Au-Yang *et al.* determined the electron band structure of Mg_2Si using empirical pseudopotential method[11].

Phonon dispersion relation of Mg_2Si was measured by neutron scattering studies at 293 K in 1988 by Hutchings *et al.*[12]. The experimental LO-TO splitting amounts to about 60 cm^{-1}. Raman scattering[13] and infrared reflectivity spectroscopy[14] measurements were also reported. Theoretical investigations using density-function theory were carried out on the phonon band structure and infrared vibrational frequencies of Mg_2Si[9,15]. The corresponding data are given in Table II.

The electrical resistivity and thermal conductivity were recently measured for Mg_2Si[16–19] and its solid solution with antimony[17,18], bismuth[16,19], silver[19] and tin[20]. We gather the transport property values for Mg_2Si into Table III. The electrical resistivity and total thermal conductivity were found to amount to about 0.07 Ω cm and 10 W m^{-1} K^{-1}, respectively. Using the Wiedemann-Franz equation, one can

estimate the electronic part of the thermal conductivity, which amounts only to about 0.1 W m^{-1} K^{-1}, i. e. around 1 % of the total thermal conductivity. Finally, it should also be mentioned that a detailed, experimental study of the lattice thermal conductivity caused by phonon-phonon scattering (normal and umklapp processes) was performed on Mg_2Ge and Mg_2Si[21]. Since we do not account for these phenomena in the present study, we will not report further on the results of this investigation.

From the literature data reported above it can be seen that, electronic and phononic structure of Mg_2Si have been investigated both by experimental and theoretical approaches. By contrast, transport properties have never been determined so far using calculation methods.

III. CALCULATION DETAILS

Density-Functional Theory approach[22,23] has been used throughout this work at the generalized gradient approximation (GGA). The Perdew-Becke-Ernzerhof (PBE) exchange and correlation functional was used[24,25]. Norm-conserving pseudopotential based on the Troullier-Martins scheme were utilised to model core electrons. The cutoff for the kinetic energy was set to 40 Hartree. The integration over the Brillouin zone was performed on a grid of k-points. The corresponding set of k-points were calculated using the Monkhorst-Pack scheme[26]. The quality of the kinetic energy cutoff and grid of k-points was tested on the calculated cell parameters and elastic constants of the Mg_2Si structure. The elastic tensor has been calculated using the Density-Functional Linear-Response Theory (DFPT)[27–30]. The formula for the shear modulus are given by the Voigt-Reuss-Hill approximations[31–33]. The best time/quality ratio was achieved with a 8^3 grid of k-points. The convergence criteria for the energy and gradients were 10^{-9} Ha and 10^{-5} Ha $bohr^{-1}$, respectively.

The EP interactions, and the thermal and electrical conductivities properties of Mg_2Si were calculated on a 24^3 grid of k-points, which amounts to a full set of 13824 k-points if one omits the time-reversal symmetry in the Brillouin zone. The DFPT method was used. We used the EP interaction theory as developped by Savrasov[34] in the realm of linear response theory. Perturbations were calculated on a set of 29 high-symmetry k-points selected among the full set of k-points, and the full integration over the Fermi surface was performed by an interpolation procedure. The calculations were performed using ABINIT package[35] (version 5.8.4).

IV. RESULTS

The calculated cell parameter is 0.6382 nm. As expected from a gradient corrected functional, our theoretical prediction is slightly overestimated, though by less than 0.5%, compared to experiment[2] (0.635 nm). Regarding the elastic constants (C_{11} = 114.5 GPa, C_{12} = 21.5 GPa, C_{44} = 45.6 GPa) and the bulk modulus (B = 52.5 GPa), excepted for the C_{11} which is underestimated by about 12 GPa, our results are in agreement with experimental data[3] (126 GPa, 26 GPa, 48.5 GPa and 49 GPa, respectively). Our predictions for the Young modulus, shear modulus and Poisson ratio are E = 107.1 GPa, G = 46.2 GPa and ν = 0.16, respectively.

As mentioned in the introduction, Mg_2Si is a semiconductor with indirect gap. The calculated electronic band structure depicted in Figure 1 shows that the gap energy at the $\Gamma_v \rightarrow X_c$ transition amounts to 0.21 eV. As expected, this value is to low compared to the experimental one (see Table I), however DFT is able to capture the essential features of the electronic band structure of Mg_2Si (see Section V). The direct band gap is predicted to amount to 1.75 eV (Exp. 2.27 eV). On Figure 2 are

depicted the DOS projections on silicon and magnesium atoms (Figure 2a), on the s, p, d and f channels of silicon (Figure 2b), and on the s, p, d and f channels of magnesium (Figure 2c). The s bands are located below -2.5 eV. The valence band near the Fermi level is largely dominated by the p orbitals, the silicon contribution prevailing over that of magnesium. In the conduction band both the silicon and magnesium contribute to roughtly the same amount. Concerning the bottom of the conduction band, between 5 and 7 eV, the s, p and d orbitals of silicon have roughtly that same statistical weight, and they combine mostly with the s orbitals of magnesium, and to a lower extend with the p and d ones. At higher energies, *i.e.* above 7 eV, the p orbitals of Mg and Si dominate the DOS. We can notice that the s orbitals of magnesium still contribute significantly to the DOS compared to the d ones up to about 9 eV. Above this threshold the s and d orbital contributions are reversed.

The phonon band structure of Mg_2Si has been calculated using perturbation theory and is depicted in Figure 3. Since the primitive unit cell contains only three atoms, nine phonon bands have been calculated at a set of special k-points with high symmetry. A Fourier interpolation scheme has been used to build the whole band structure. At the Γ k-point the bands feature an optical branch which is threefold degenerate at 7.61 THz. At higher frequencies, the second optical branch, which should also be threefold degenerate, is split by the macroscopic electric field into a low-lying, twofold transverse optical mode at 8.03 THz and a single, high-lying longitudinal optical mode at 9.98 THz. Therefore, the LO-TO splitting amounts to 1.95 THz (65 cm^{-1}) which is in good agreement with experimental data (60 cm^{-1}) and other theoretical predictions (see Table II). In Figure 4 is depicted the phonon density of states (ph-DOS) and the corresponding DOS projected onto the magnesium and silicon atoms. The peak of the ph-DOS centered at around 8.5 THz is dominated by the states pertaining to the magnesium vibrational modes whereas the

modes below 7.5 THz and above 9 THz belong mostly to the silicon atom vibrational modes.

Using the Savrasov formalism we calculated by response theory the electrical resistivity and electronic thermal conductivity. The results are presented in Table III. We note that the electrical resistivity is too low compared to experimental measurements by about two orders of magnitudes. By contrast, the calculated electronic thermal conductivity is overestimated. The reason for these discrepancies is explained in the next section. The electron-phonon interaction is one of the key quantity to explain transport properties. The Eliashberg spectral function $\alpha^2F(\omega)$ and the spectral transport function $\alpha^2F_{\rm tr}(\omega)$ are depicted on Figure 5. The Eliashberg function does not differ significantly from the transport function, the latter being only slightly less intense than the former. Therefore we only describe the transport function. A broad peak is observed at low frequency that span from about 1 THz to 4 THz. Then four peaks are depicted: the less intense one is centrered at 5.8 THz, then a broader peak is centrered at 7 THz, and two sharp peaks are found at 8.5 THz and 9.9 THz, the latter one being the most intense one over the whole spectrum.

V. DISCUSSION

The electronic band structure depicted in Figure 1 shows that, at the Γ (0,0,0) k-point the Fermi state is threefold degenerate whereas the first conduction state is not degenerate and the second one is threefold degenerate. This feature is also observed when using the Perdew-Wang (PW91) exchange-correlation GGA functional[9]. By contrast, the band structure is different at the Hartree-Fock (HF) and hybrid (HF+DFT using the adiabatic connection) theoretical levels[9]. In effect, at the Hartree-Fock level the first conduction state is threefold degenerate at the Γ k-point.

When mixing Hartree-Fock with the PW91 functional, the first conduction state becomes twofold degenerate only. Hence, as expected, the admixture of electronic correlation into the hamiltonian tends to correct, at least partially, the Hartree-Fock deficiencies, though not enough to yield a correct picture of the conduction band. In addition, the band gap is still to high (about the same in magnitude as the HF one). Note that our description of the electronic band structure is also consistent with that of D. M. Wood and A. Zunger[36] and M. Y. Au-Yang and M. L. Cohen[11] whom used perturbation theory and empirical pseudopotential approaches, respectively.

Although DFT provides a qualitatively satisfactory description of the electronic band structure of Mg_2Si, we believe that, the misfit between the calculated energy gap and the experimental one leads to wrong estimates of the electrical and electronic thermal conductivities, as we shall see. At first sight, the discrepancies could be explained by noting that, several effects are neglected in the calculations, namely, the electron-electron diffusion and the thermal activation. Both effects can increase the electrical resistivity of Mg_2Si. However, the bad description of the electronic gap may also play a important role. Indeed, if we assume that, Mg_2Si behaves as a semi-conductor, the resistivity should vary with the temperature according to the exponential law: $\rho(T) = \rho_0 \exp(\frac{E_g}{2kT})$. Therefore, we have at 300 K, using data from Table I: $E_{g,\text{calc.}} = E_{g,\text{exp.}} + 2kT \ln \frac{\rho_{\text{calc.}}}{\rho_{\text{exp.}}} = 0.46$ eV. We see that the gap is significantly improved, by a factor of two. As a consequence, improving the electronic gap should significantly increase the resistivity of Mg_2Si. The prediction of the gap energy could be improved by implementing a scissors operator or by performing GW calculations, though the latter option would be computationally too expensive.

In order to understand the electron-phonon (EP) interactions in the case of Mg_2Si, we show in Figure 6 both the phonon DOS projected onto the Mg and Si atoms

and the transport spectral function $\alpha^2 F_{tr}(\omega)$. One can see that the EP coupling is generally stronger for frequencies corresponding to vibrational modes in which the contribution of silicon prevails. The only exception is for ν =8.4 THz where the contribution of Mg atoms is slightly larger than that of Si one. This could explain why the replacement of silicon atoms by heavier ones (e.g. Sb, Bi, Ag, Sn)[17,18,20] improves the Mg_2Si thermoelectric properties. Heavy atoms lead to a reduction of atomic vibrations, and as a consequence to a decrease of the trapping of charge carriers which is large when EP interactions are strong[37]. In addition, the introduction of heavy atoms into the Mg_2Si lattice increases phonon scattering and therefore, reduces the lattice thermal conductivity.

VI. CONCLUSION

In this work we studied the electronic, vibrational and EP coupling properties of the Mg_2Si compound.

The features of the electronic band structure agree with previous calculations obtained with different exchange-correlation functional. However, the DFT approach improves the description of the electron bands over the Hartree-Fock and hybrid Hartree-Fock-DFT approaches. The gap energy calculated by pure DFT method is much too small compared to experimental findings and to GW calculations. The electrical resistivity is also too low compared to experimental data. We infered that the discrepancy between the calculated and experimental electrical resistivity is related to the underestimation of the gap energy.

The EP coupling was found to be stronger for frequencies corresponding mainly to silicon vibrational modes. This phenomenon could be at the origin of the improvement

of the thermoelectric properties of Mg_2Si by designing solid solutions.

---

* Corresponding author: pascal.boulet@univ-provence.fr

[1] V. K. Zaitsev, M. I. Fedorov, I. S. Eremin, and E. A. Gurieva, *Thermoelectrics Handbook: Macro to Nano-Structured Materials* (New York: CRC press, 2006).

[2] J. G. Barlock and L. F. Mondolfo, Zeitschrift Für Metallkunde **66** (1975).

[3] O. Madelung, in *Landbolt-Börnstein Numercal Data and Functional Relationships in Science and Technology, New Series, Group III*, Vol. 17e (Springer-Verlag, Berlin, 1983) pp. 163, 432.

[4] U. Winckler, Helv. Phys. Acta **28**, 633 (1955).

[5] R. G. Morris, R. D. Redin, and G. C. Danielson, Phys. Rev. **109**, 1909 (1958).

[6] P. Koenig, D. Lynch, and G. Danielson, J. Phys. Chem. Sol. **20**, 122 (1961).

[7] F. Vazquez, R. A. Forman, and M. Cardona, Phys. Rev. **176**, 905 (1968).

[8] P. M. Lee, Phys. Rev. **135**, A1110 (1964).

[9] P. Baranek and J. Schamps, J. Phys. Chem. B **103**, 2601 (1999).

[10] B. Arnaud and M. Alouani, Phys. Rev. B **64**, 033202 (2001).

[11] M. Y. Au-Yang and M. L. Cohen, Phys. Rev. **178**, 1358 (1969).

[12] M. T. Hutchings, T. W. D. Farley, M. A. Hackett, W. Hayes, S. Hull, and U. Steigenberger, Sol. State Ion. **28-30**, 1208 (1988).

[13] C. J. Buchenauer and M. Cardona, Phys. Rev. B **3**, 2504 (1971).

[14] D. McWilliams and D. W. Lynch, Phys. Rev. **130**, 2248 (1963).

[15] J. ichi Tani and H. Kido, Comput. Mater. Sci. **42**, 531 (2008).

[16] J. ichi Tani and H. Kido, Phys. B **364**, 218 (2005).

[17] J. ichi Tani and H. Kido, Interm. **15**, 1202 (2007).

[18] G. S. Nolas, D. Wang, and M. Beekman, Phys. Rev. B **76**, 235204 (2007).

[19] M. Akasaka, T. Iida, A. Matsumoto, K. Yamanaka, Y. Takanashi, T. Imai, and N. Hamada, J. Appl. Phys. **104**, 013703 (2008).

[20] V. K. Zaitsev and M. I. Fedorov, Semicond. **29**, 490 (May 1995).

[21] A. H. Awad and K. S. Dubey, J. Therm. Anal. **24**, 233 (1982).

[22] P. Hohenberg and W. Kohn, Phys. Rev. **136**, B864 (1964).

[23] W. Kohn and L. J. Sham, Phys. Rev. **140**, A1133 (1965).

[24] J. Perdew, K. Burke, and M. Ernzerhof, Phys. Rev. Lett. **77**, 3865 (1996).

[25] J. Perdew, K. Burke, and M. Ernzerhof, Phys. Rev. Lett. **78**, 1396 (1997).

[26] H. J. Monkhorst and J. D. Pack, Phys. Rev. B **13**, 5188 (1976).

[27] X. Gonze, Phys. Rev. A **52**, 1096 (1995).

[28] X. Gonze, Phys. Rev. B **55**, 10337 (1997).

[29] X. Gonze and C. Lee, Phy. Rev. B **55**, 10355 (1997).

[30] S. Baroni, S. de Gironcoli, A. D. Corso, and P. Giannozzi, Rev. Mod. Phys. **73**, 515 (2001).

[31] W. Voigt, *Lehrbuch der Kristallphysiks* (B. B. Teubner, Leipzig, 1928).

[32] A. Reuss, Z. Angew. Math. Mech. **9**, 49 (1929).

[33] R. Hill, Proc. Phys. Soc. **65**, 349 (1952).

[34] S. Y. Savrasov, Phys. Rev. B **54**, 16470 (1996).

[35] X. Gonze, B. Amadon, P. Anglade, J. Beuken, F. Bottin, P. Boulanger, F. Bruneval, D. Caliste, R. Caracas, M. Côté, T. Deutsch, L. Genovese, P. Ghosez, M. Giantomassi, S. Goedecker, D. Hamann, P. Hermet, F. Jollet, G. Jomard, S. Leroux, M. Mancini, S. Mazevet, M. Oliveira, G. Onida, Y. Pouillon, T. Rangel, G. Rignanese, D. Sangalli, R. Shaltaf, M. Torrent, M. Verstraete, G. Zerah, and J. Zwanziger, Comput. Phys. Comm. **180**, 2582 (2009).

[36] D. M. Wood and A. Zunger, Phys. Rev. B **34**, 4105 (1986).

[37] D. Emin, *Thermoelectrics Handbook: Macro to Nano-Structured Materials* (New York: CRC press, 2006).

Table I. Experimental (300 K) and calculated electronic properties of Mg_2Si.

Property	Calc. (from literature)	Calc. (this work)	Exp.
Direct gap $\Gamma_v \rightarrow \Gamma_c$ (eV)	1.55[a][10],1.65[b][9], 2.20[c][10]	1.75	2.27[7]
Indirect gap $\Gamma_v \rightarrow X_c$ (eV)	1.3[d][8] 0.12[a][10], 0.65[c][10]	0.21	0.66–0.78[4–6]
Effective mass $m_{\parallel}/m_0$	0.69[8]	0.58	–
Effective mass $m_{\perp}/m_0$	0.25[8]	0.19	–

[a] LDA functional.

[b] GGA functional.

[c] GW calculations.

[d] Empirical pseudopotential.

Table II. Experimental and calculated phonon frequencies of Mg_2Si.

Property	Calc. (from literature)	Calc. (this work)	Exp.
Phonon modes $\Delta_2^{'}, \Delta_5$ (TO) (THz)	7.94[9], 7.70[15]	7.61	7.73[12,13]
Phonon mode Δ_5 (TO) (THz)	8.06[9], 8.18[15]	8.03	7.97[12], 8.00[14]
Phonon mode Δ_1 (LO) (THz)	10.04[15]	9.98	9.77[12], 9.80[14]

Table III. Electrical resistivity and thermal conductivities of Mg_2Si at 300 K.

Property	Calc. (this work)	Exp.
Electrical resistivity $\rho(\Omega$ cm)	$5.47\ 10^{-4}$	$7.14\ 10^{-2}$ [16,17], $7.16\ 10^{-2}$ [18]
Total thermal conductivity κ(W cm^{-1} K^{-1})	–	0.105[16,17], 0.095[19]
Electronic thermal conductivity κ_{el}(W cm^{-1} K^{-1})	0.0123 (0.0134[a])	$\leq 10^{-3}$ [16,17], 0.002[19]

[a] Using Wiedemann-Franz law: $\kappa_{el} = L_0 \sigma T$ with $L_0 = 2.44\ 10^{-8}$ V^2 K^{-1}

FIGURE CAPTIONS

Figure 1: Electronic band structure of Mg_2Si calculated with the PBE density functional.

Figure 2a: Total electron density of states (DOS) and and DOS projected on magnesium and silicon atoms. Legend: $-$ total DOS; $--$ Si contribution; $-\cdot$ Mg contribution.

Figure 2b: Electron density of states projected on the s, p, d and f channels of silicon. Legend: $-$ Si total contribution; $--$ s; $-\cdot$ p; $-\cdot\cdot$ d; $\cdot--$ f.

Figure 2c: Electron density of states projected on the s, p, d and f channels of magnesium. Legend: $-$ Mg total contribution; $--$ s; $-\cdot$ p; $-\cdot\cdot$ d; $\cdot--$ f.

Figure 3: Phonon band structure of Mg_2Si.

Figure 4: Phonon density of state and contribution of silicon and magnesium atoms.

Figure 5: Eliashberg function $\alpha^2F(\omega)$ and transport spectral function $\alpha^2F_{tr}(\omega)$.

Figure 6: Contribution of silicon and magnesium atoms to the phonon density of state and transport spectral function $\alpha^2F_{tr}(\omega)$. Legend: $-$ transport spectral function $\alpha^2F_{tr}(\omega)$; $--$ Si contribution to the phonon DOS; $-\cdot$ Mg contribution to the phonon DOS.

Figure 1

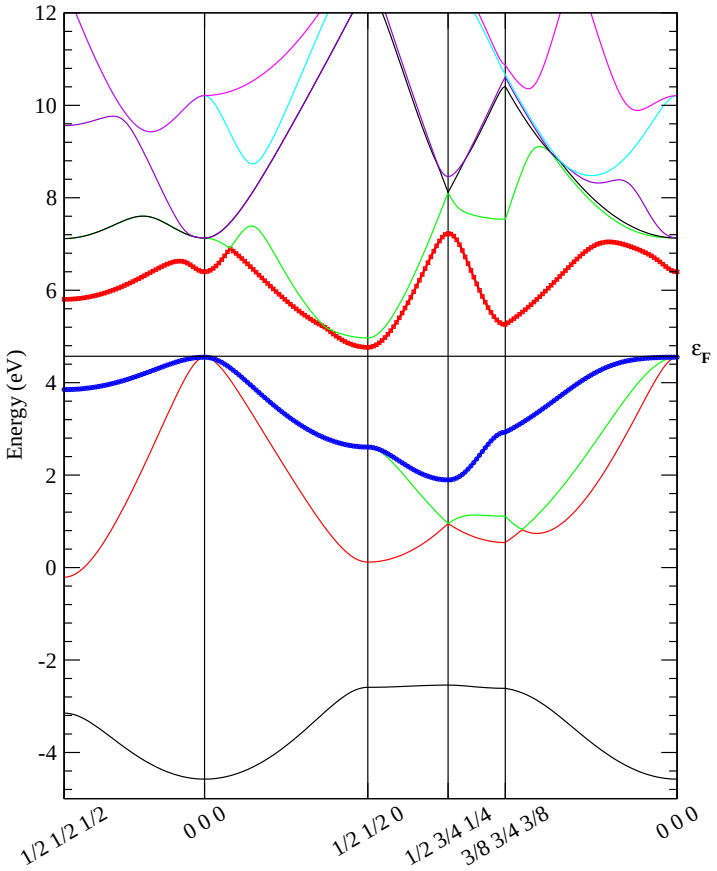
12
10
8
6
4
2
0
-2
-4
Energy (eV)
ε_F
1/2 1/2 1/2
0 0 0
1/2 1/2 0
1/2 3/4 1/4
3/8 3/4 3/8
0 0 0

Figure 2a

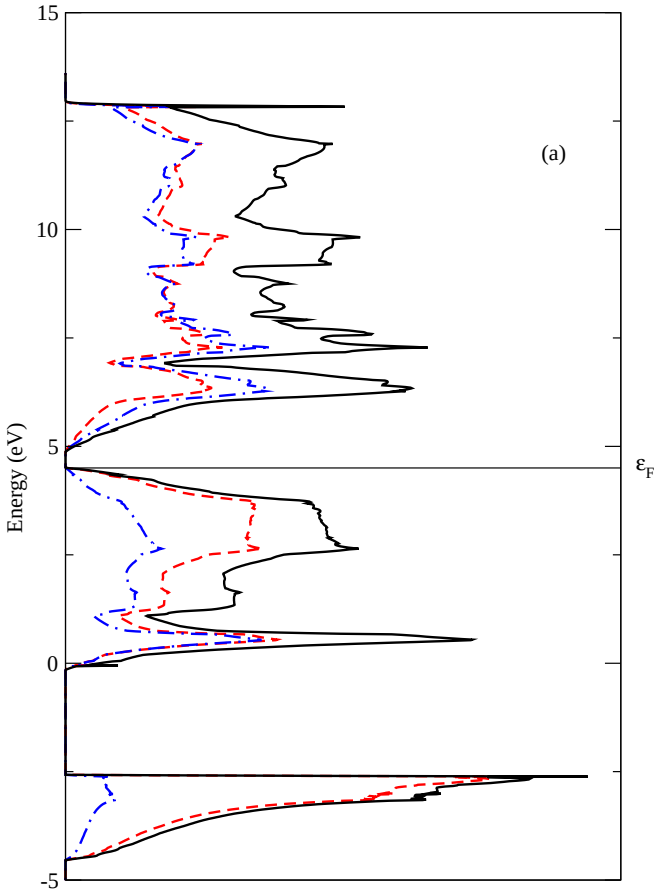

Figure 2b

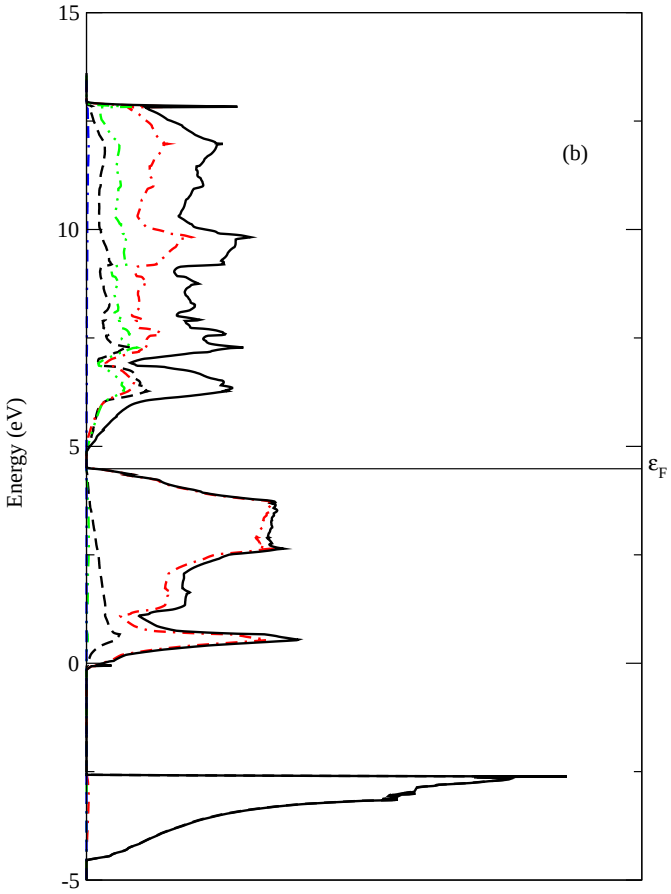

Figure 2c

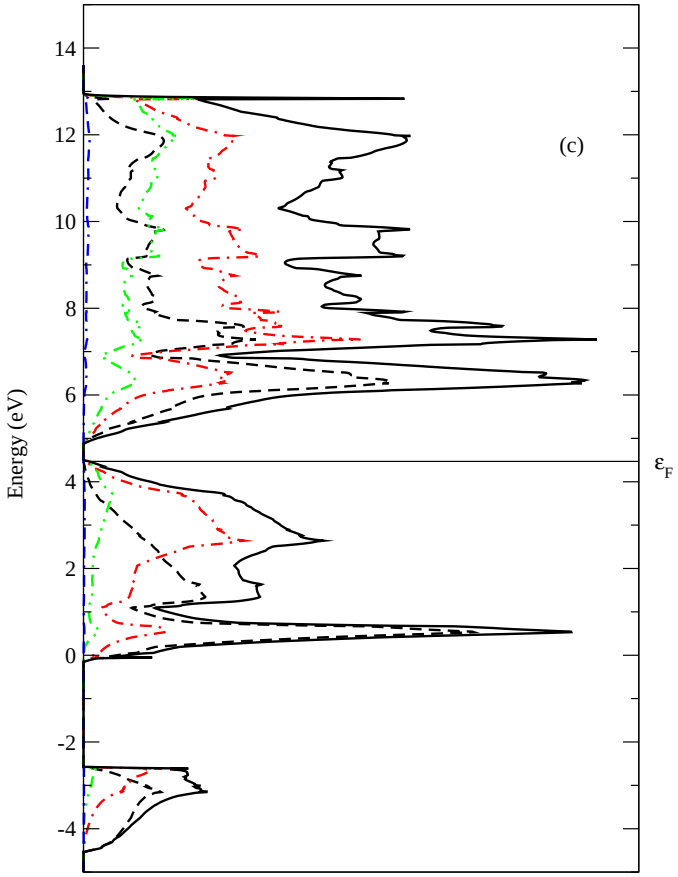

Figure 3

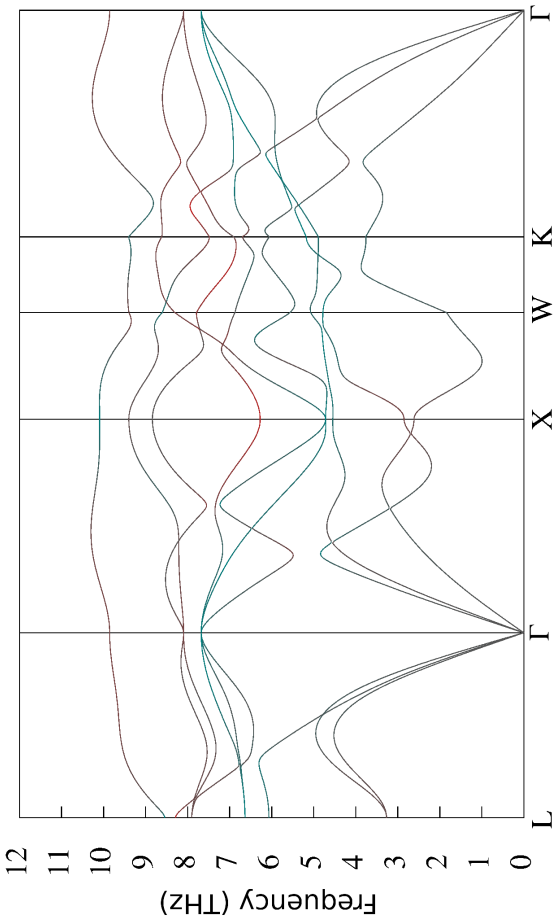

Figure 4

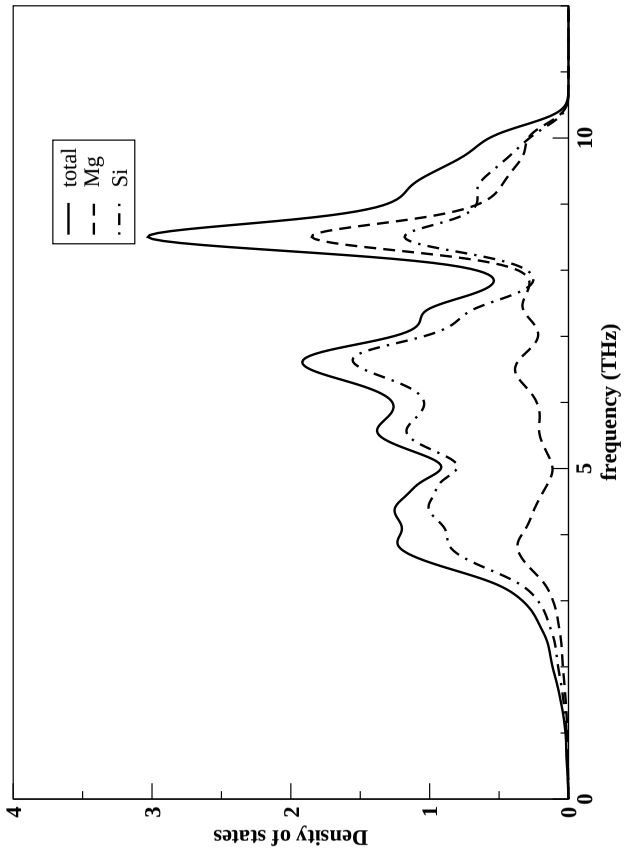

Figure 5

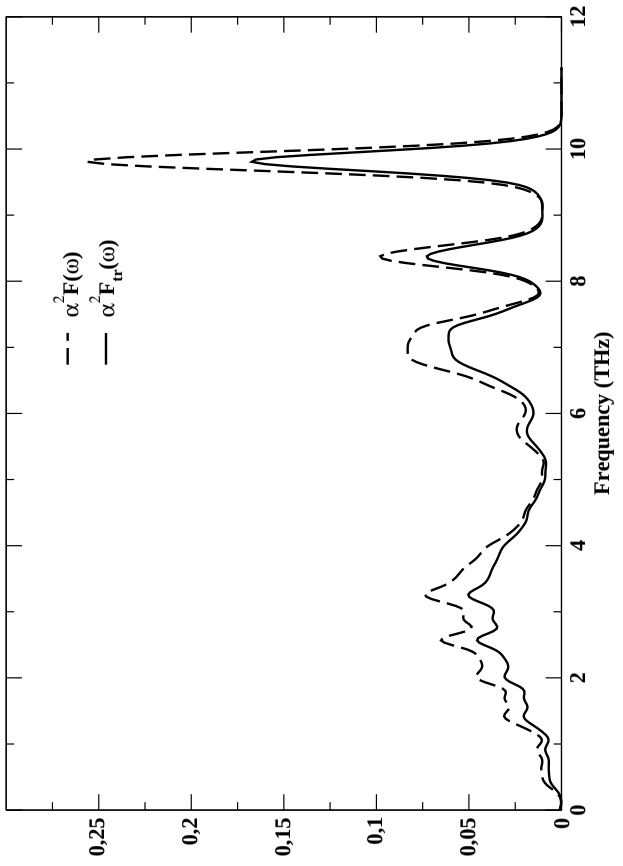

Figure 6